

## From precision nuclear structure information to constraining statistical properties: Methodical developments in photonuclear reactions

D. SAVRAN<sup>(1)</sup>, J. ISAAK<sup>(2)</sup>, A. D. AYANGEAKAA<sup>(3)(4)</sup>, M. BEUSCHLEIN<sup>(2)</sup>,  
S. W. FINCH<sup>(4)(5)</sup>, D. GRIBBLE<sup>(2)</sup>, A. GUPTA<sup>(2)</sup>, J. HAUF<sup>(2)</sup>, X. K. JAMES<sup>(3)(4)</sup>,  
R. V. F. JANSSENS<sup>(3)(4)</sup>, S. R. JOHNSON<sup>(3)(4)</sup>, P. KOSEOGLOU<sup>(2)</sup>,  
T. KOWALEWSKI<sup>(3)(4)</sup>, B. LÖHER<sup>(1)</sup>, O. PAPST<sup>(2)</sup>, N. PIETRALLA<sup>(2)</sup>,  
A. SARACINO<sup>(3)(4)</sup>, N. SENSHARMA<sup>(3)(4)</sup>, W. TORNOW<sup>(4)(5)</sup> and V. WERNER<sup>(2)</sup>

<sup>(1)</sup> *GSI Helmholtzzentrum für Schwerionenforschung - Darmstadt, Germany*

<sup>(2)</sup> *Institute for Nuclear Physics, Technische Universität Darmstadt - Darmstadt, Germany*

<sup>(3)</sup> *Department of Physics and Astronomy, University of North Carolina - Chapel Hill, NC, USA*

<sup>(4)</sup> *Triangle Universities Nuclear Laboratory - Durham, NC, USA*

<sup>(5)</sup> *Department of Physics, Duke University - Durham, NC, USA*

received 31 October 2023

**Summary.** — We report on a new method to perform nuclear self-absorption measurements in combination with a monochromatic photon beam produced via laser Compton backscattering. We have used the method for two very different applications: The precision determination of the transition width of the first excited state in <sup>12</sup>C to the ground state and to determine nuclear level densities up to the neutron separation energy in <sup>88</sup>Sr. Both experiments serve as a proof of principle and are currently being analyzed. First preliminary results are presented.

### 1. – Introduction

Photon-induced reactions have been one of the working horses in nuclear physics to determine properties of low-spin excited states of atomic nuclei [1]. Below particle thresholds, the nuclear resonance fluorescence (NRF) reaction allows for a model-independent determination of level energies, spin and parity quantum numbers as well as transition probabilities and has been extensively used (in combination with other methods) to provide data on the so-called pygmy dipole resonance (see, *e.g.*, the reviews [1-3]).

In standard NRF experiments, energy-integrated cross sections, that are linked to transition probabilities, are usually determined relative to a well-known standard, see, *e.g.*, [4] for the combined analysis of NRF data obtained with both bremsstrahlung and monochromatic beams using laser Compton backscattering (LCB). In contrast, the method of nuclear self-absorption overcomes the need of a calibration reactions. In these

experiments, the reaction cross section is extracted by determining the probability of absorption of photons at the resonance energy. This is achieved by comparing the number of NRF reactions in a scattering target (short *scatterer*) in two experiments: one with an absorber target (short *absorber*) before the scattering target and one without the absorber. A difficulty of these experiments is the normalization of the two measurements to each other. This has been overcome in an extension of the method called relative self-absorption (RSA) in combination with bremsstrahlung photon beams [5]. The RSA technique strongly reduced systematic uncertainties and allows to determine cross sections with high precision. A further extension of the method to allow RSA experiments also with monochromatic photon beams produced via LCB was recently proposed in [6]. Here we report on the first experiments using the new method for two different physics cases: The precise determination of the  $B(E2, 0_1^+ \rightarrow 2_1^+)$  value in  $^{12}\text{C}$  and the determination of level densities below the particle threshold in  $^{88}\text{Sr}$ .

**1.1. Precision measurements of transition widths.** – A lot of effort is put into modern nuclear theory providing refined calculations of ground-state properties and electromagnetic observables in light nuclei. A set of ab-initio many-body methods that probe ground-state and excitation energies as well as spectroscopic observables in p- and lower sd-shell nuclei are the no-core shell model [7,8,8,9] and the importance truncated no-core shell model (IT-NCSM) [10,11]. To benchmark such calculations that provide very precise predictions, experimental data with sufficient small uncertainties is needed. A recent example is given in [12], where a precise determination of the  $B(M1, 1_1^+ \rightarrow 0_1^+)$  value in  $^6\text{Li}$  via the RSA technique allowed to demonstrate the importance of two-body currents that enter at next-to-leading order in ab-initio calculations based on chiral effective field theory. In this example, the state of interest has a very large photo-excitation cross section due to the large ground state width of the  $0_1^+$  state in  $^6\text{Li}$ . For such strongly excited states sufficient precision can be reached in RSA experiments with bremsstrahlung.

As one of the major benchmark nuclei for modern nuclear theory,  $^{12}\text{C}$  was studied in numerous theoretical approaches (see, *e.g.*, [13,14] and references therein). The prediction and description of ground-state properties and electromagnetic observables in the light-mass many-body system of  $^{12}\text{C}$  presents a challenge for nuclear theory. In the past years, of particular interest is the correlation between the  $B(E2)$  transition strength from the  $2_1^+$  state to the  $0_1^+$  ground state and the quadrupole moment (Q) of the  $2_1^+$  that was studied, *e.g.*, by Calci *et al.* in [14]. In order to constrain such correlations and the nuclear models, a precise measurement of the  $B(E2)$  value is needed and the RSA method is well suited for this challenge.

However, in this case the excitation cross section is a factor of 800 smaller compared to the one in [12]. For weaker excitations, such as the  $2_1^+$  in  $^{12}\text{C}$  the use of a mono-energetic photon beam provides much better sensitivity by a strongly reduced background compared to experiments with bremsstrahlung. The extension of the RSA method to LCB beams proposed in [6] allows to determine cross sections to very high precision, independent from any calibration standard. We therefore chose  $^{12}\text{C}$  as the first case to demonstrate the power of the RSA method in combination with a LCB photon beam.

**1.2. Determination of level densities.** – One of the most important approaches to model nuclear reactions is the Hauser-Feshbach formalism [15], which treats compound nuclear reactions in a statistical fashion. It is applied in regions where the properties of individual nuclear resonances are not well known or cannot be studied separately. Thus, instead of probing individual nuclear excited states, average quantities are defined to

quantify the properties of atomic nuclei. One such quantity is the nuclear level density (NLD) which specifies the number of nuclear levels for a given energy interval. Another crucial quantity related to the  $\gamma$  decay of the nucleus is the photon strength function (PSF). Its concept is based on the assumption that at excitation energies of high NLD, the PSF describes the average probability of absorption and emission of electromagnetic radiation by the nucleus. In addition to the average quantities defined for an ensemble of nuclear resonances such as NLDs and PSFs, fluctuation properties of this ensemble represent an important foundation of the statistical model.

To date, most of the values on NLD have been extracted from neutron resonances data (see, *e.g.*, refs. [16-18]), which is restricted to energies just above the neutron separation energy. At low excitation energies NLDs can be determined via complete spectroscopy, however, at these low NLDs the statistical model is not applicable anyway. At excitation energies in between only little is known on absolute values for NLDs. The functional forms of NLDs and PSFs in the region in between have been determined, *e.g.*, from light-ion reactions using the Oslo method [19,20], but the applied analysis technique heavily depends on the validity of the Brink-Axel hypothesis and on the correct treatment of the spin window populated in the corresponding reactions [21].

The method of nuclear self-absorption offers a completely new approach to determine NLD in the energy below the neutron separation energy. For a given integrated photo-absorption cross section in a defined excitation energy interval the amount of self-absorption depends on the number of levels in that interval. The details of the method are explained below. We have chosen  $^{88}\text{Sr}$  as a first candidate to apply the new method.

## 2. – RSA with mono-energetic photon beams

The basic idea of nuclear self-absorption is to investigate the absorption spectrum within the photon beam used and to determine the NRF reaction cross section by the depth of the absorption lines. The upper part of fig. 1 illustrates schematically the effect of absorption within a thick absorber on the energy profile of the photon beam. While atomic absorption smoothly reduced the photon intensity over the full energy region the nuclear absorption produced characteristic absorption lines. However, bound nuclear resonances usually exhibit very narrow width in the meV to eV range. Thus, absorption lines cannot be resolved with state-of-the-art  $\gamma$ -ray detectors. This can be overcome by using the nucleus of interest itself as a high-resolution detector: The amount of photons that are absorbed within the absorber is analyzed by irradiating a scattering target of the same material placed behind the absorber. The effect on the spectrum emitted from the scattering target is shown in the lower part of fig. 1 (filled peaks). The comparison between a measurement with absorber and without then allows to determine the reduction of NRF reactions due to the total absorption. In order to extract the nuclear contribution the atomic attenuation has to be accounted for. Within the method of RSA proposed in [5], a reference material is added to the scattering target. Since this material is not present in the absorber target, the reduction of the intensity of its NRF lines is only due to atomic attenuation. Thus, these NRF peaks (dashed in fig. 1) can be used to normalize the measurement with and without absorber to each other, and automatically account for the atomic attenuation (and any other factor such as dead times). This method of normalization offers very small systematic uncertainties and has been used in the case of  $^6\text{Li}$  to determine the B(M1) of the first excited  $0^+$  state to a precision of less than 2% using bremsstrahlung [12].

One of the great advantages of scattering experiments with LCB photon beams is the

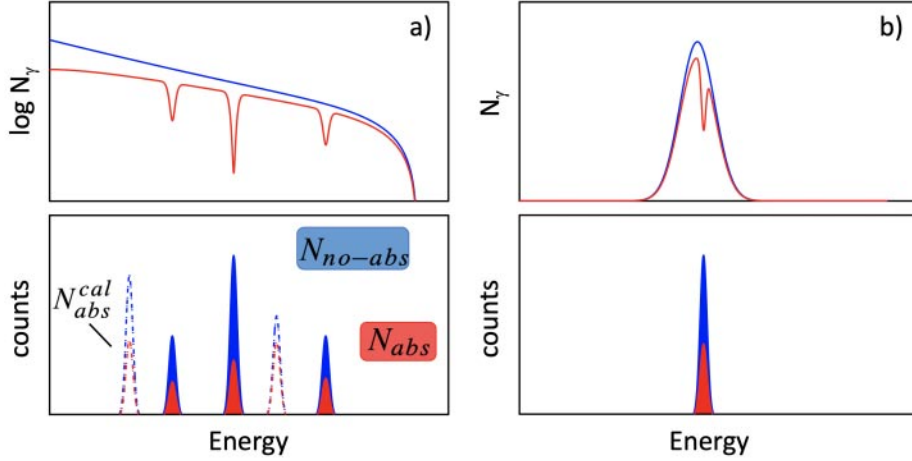


Fig. 1. – Schematic illustration of the effect of atomic and nuclear absorption on the photon beam and the NRF spectra for bremsstrahlung (a) and LCB (b).

strongly reduced background in the energy region of interest compared to experiments with bremsstrahlung. Therefore, the sensitivity for self-absorption experiments is better and transition-width measurements with higher precision are feasible. In addition, integrated quantities, such as the total integrated cross section can be studied using LCB beams (see, *e.g.*, [22-25]).

The novel idea of RSA experiments with quasi-monochromatic photon beams at the High Intensity  $\gamma$ -ray Source (HI $\gamma$ S) [26] at Duke University has been proposed in [6] and only a short summary will be given in the following. The schematic layout of the self-absorption experiment performed at HI $\gamma$ S is shown in fig. 2. Two experimental setups have been used, one before and one after the absorber targets. At the first target position (T1) the unperturbed LCB photon beam irradiates a thin target with the isotope of interest. Behind T1, a thick absorber of the element of interest is placed into the photon beam producing the characteristic absorption dips in the energy profile of the photon beam, as shown schematically in fig. 1. As outlined before, the overall photon intensity is reduced by atomic attenuation in the absorber. Afterwards, the modified photon beam irradiates a second thin target of at T2.

As shown in [6, 27] the low-energy part of the spectrum (and in particular the 511-keV annihilation peak) is proportional to the integrated photon intensity. Thus, for each individual detector the intensity of the 511-keV line can be used to normalize the number of observed NRF reactions, which is determined by the intensity of the corresponding NRF peak. This normalization also accounts for any kind of dead time or pile-up, since both peak intensities are extracted from the same spectrum.

In the present experiment, two sets of measurements have been performed, one without the absorber and one with the absorber in place. For each measurement the observed NRF reactions in both setups have been normalized to the 511-keV peaks of the corresponding detectors, thus normalizing to the integrated photon intensity at T1 and T2 individually. Therefore, this procedure accounts for the reduction of the photon intensity

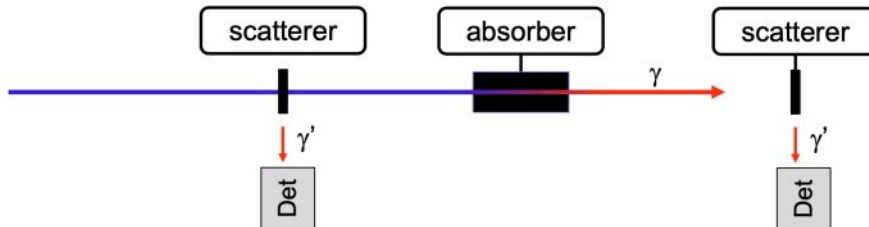


Fig. 2. – Schematic view of the RSA experiment. Between two NRF setups the absorber target is placed (well shielded from the detector setups). Comparing the number of NRF reactions in the two setups allows to determine the excitation cross section.

due to atomic attenuation at T2. The self-absorption coefficient  $R$  is then given by

$$(1a) \quad R = 1 - \frac{N_{abs}^{T2}/N_{abs}^{T1}}{N_{no-abs}^{T2}/N_{no-abs}^{T1}}$$

with  $N_{abs,no-abs}^{T1,T2}$  being the normalized NRF intensities at T1 and T2 with and without absorber, respectively. Taking these double ratios also corrects for any possible shift of the beam energy. Overall the normalization procedure and the use of two NRF setups minimizes the systematic uncertainties.

Figure 3 shows spectra of one HPGe and one LaBr detector at T2 for the case of  $^{12}\text{C}$ . For all spectra, the energy of the photon beam was centered at the excitation energy of the  $2_1^+$  state at 4.44 MeV, with an energy spread of about 3%. Thus, only the  $2_1^+$  state is excited and its decay is the only NRF peak observed in the spectrum. Besides spectra with and without absorber target also spectra without scattering targets at T2 are shown. The low background conditions at 4.44 MeV demonstrate the high sensitivity of the method. The spectra without any scattering target show that background contributions to the 511-keV peak are on the  $10^{-3}$  level.

### 3. – Precision measurement of the $B(E2, 0_1^+ \rightarrow 2_1^+)$ value

The first RSA experiment performed with the new method was performed at the end of 2022 to measure the  $B(E2, 0_1^+ \rightarrow 2_1^+)$  in  $^{12}\text{C}$  to a precision of about 2%. Beside the determination of the transition width a focus was set on the investigation of systematic uncertainties by different sets of measurements. In addition to the runs with  $^{12}\text{C}$  scattering targets also measurements without scattering targets were performed, as explained above. In order to test the reliability of the normalization via the 511-keV peak, runs with high statistics using  $^{11}\text{B}$  scattering targets have been performed. The resonances at 4444 keV in  $^{11}\text{B}$  is strongly excited in NRF, and because it is not effected by the nuclear absorption of the carbon absorber, provides an ideal test of the normalization procedure with high precision. In addition, measurements have been performed with two LaBr detector placed directly into the photon beam, one set with carbon absorber in-between and on set without. The comparison of the two sets, thus, provides another measurement of the atomic absorption within the carbon absorber target.

The analysis of the data is still ongoing. The preliminary value for the nuclear self absorption has been determined to be  $R = 0.4009(46)$  when using the normalization via

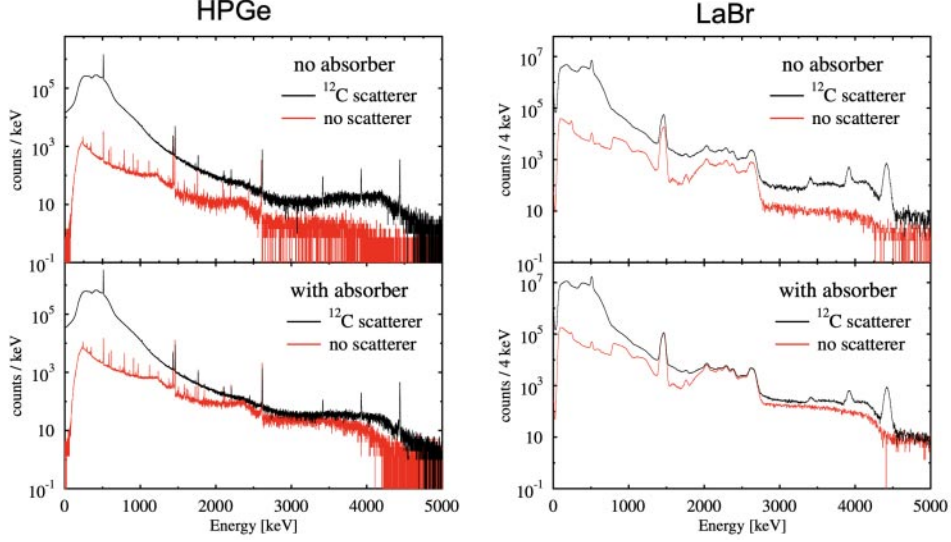


Fig. 3. – Measured spectra for the different experimental settings. In addition, spectra for measurements without scattering target are shown, illustrating the low background conditions.

the 511-keV peak. Based on the value for the self absorption a value of 11.05(19) meV is extracted for the decay width of the  $2^+$  state. Just recently, the results of a high-precision measurement using electron scattering at the S-DALINAC at TU Darmstadt has been published [28]. There a value 10.61(26) meV is reported. Both values are in good agreement within the given statistical uncertainties, even though they have been extracted via completely different methods.

#### 4. – Level density in $^{88}\text{Sr}$

As the nuclear level density increases the analysis of isolated transitions becomes difficult. Therefore, we have developed an integral approach to extract nuclear structure information such as the average photo-excitation cross section also in the region of medium to high NLD within NRF experiments using LCB photon beams (see, *e.g.*, [4] and references therein).

The method to extract the NLD from this kind of data is based on the fact, that for a given integrated cross section in an excitation energy interval the nuclear absorption depends on the number of levels within this interval: For a higher level density the average cross section of the individual levels is smaller (since the integral is fixed) yielding a small nuclear absorption. Thus, for a given integrated cross section a correlation between the NLD and the self-absorption factor  $R$  can be evaluated, as shown in the left part of fig. 4 for the case of  $^{88}\text{Sr}$  at an excitation energy of 8.6 MeV for three different absorber thicknesses. To calculate this correlation, a distribution for the level widths has to be assumed, which is usually done using the so-called Porter-Thomas (PT) distribution [16]. The effect of different distributions and details on the method have been evaluated in [29].

The nuclear self-absorption  $R$  as well as the integrated cross section are extracted from the experimental spectra after accounting for the detector response using the unfolding

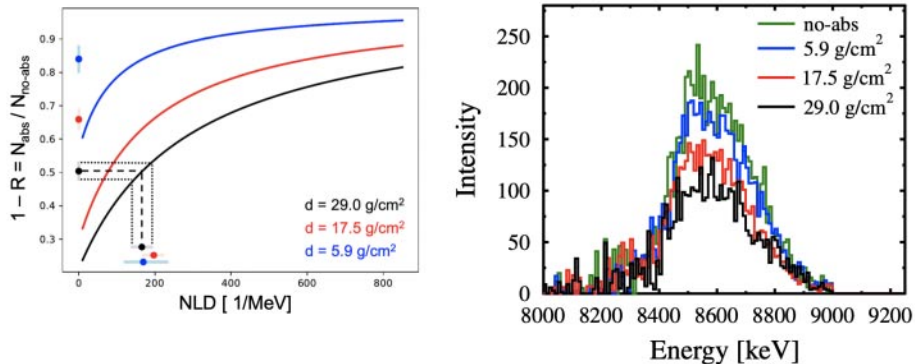


Fig. 4. – Left side: Correlation between NLD and measured nuclear self-absorption for three different absorber thicknesses and an excitation energy of 8.6 MeV. Right side: Measured  $\gamma$ -ray spectra of a LaBr detector at T2 after accounting for the detector response. Integration of the spectra and taking the ratio between measurements with and without absorber yield the data points shown in the left part.

technique. Examples for spectra of a LaBr detector at the second setup are given in the right part of fig. 4, which have been used to extract the experimental values shown in the left part of the figure for  $1 - R$ . Using the correlation the NLD can be extracted for each absorber thickness individually. As can be seen, the three different values are in very good agreement for the given example.

Data has been taken in the energy region of about 5 MeV to 10 MeV. The analysis of the data is currently ongoing to extract NLD as well as cross sections for the entire energy region.

\* \* \*

The author acknowledges the HI $\gamma$ S accelerator staff for providing excellent beams and experimental conditions. This work was supported by the grant “Nuclear Photonics” within the LOEWE program of the State of Hesse, within the Research Cluster ELEMENTS (Project ID 500/10.006), and by the U.S. Department of Energy, Office of Nuclear Physics under grants No DE-FG02-97ER41033 (TUNL) and No DE-FG02-97ER41041 (UNC).

## REFERENCES

- [1] ZILGES A., BALABANSKI D., ISAAK J. and PIETRALLA N., *Prog. Part. Nucl. Phys.*, **122** (2022) 103903.
- [2] SAVRAN D., AUMANN T. and ZILGES A., *Prog. Part. Nucl. Phys.*, **70** (2013) 210.
- [3] BRACCO A., CRESPI F. C. L. and LANZA E. G., *Eur. Phys. J. A*, **51** (2015) 99.
- [4] ISAAK J., SAVRAN D., LÖHER B., BECK T., FRIMAN-GAYER U., KRISHICHAYAN, PIETRALLA N., PONOMAREV V. Y., SCHECK M., TORNOW W., WERNER V., ZILGES A. and ZWEIDINGER M., *Phys. Rev. C*, **103** (2021) 044317.
- [5] ROMIG C., SAVRAN D., BELLER J., BIRKHAN J., ENDRES A., FRITZSCHE M., GLORIUS J., ISAAK J., PIETRALLA N., SCHECK M., SCHNORRENBERGER L., SONNABEND K. and ZWEIDINGER M., *Phys. Lett. B*, **744** (2015) 369.
- [6] SAVRAN D. and ISAAK J., *Nucl. Instrum. Methods Phys. Res. A*, **899** (2018) 28.

- [7] BARRETT B. R., NAVRÁTIL P. and VARY J. P., *Prog. Part. Nucl. Phys.*, **69** (2013) 131.
- [8] NAVRÁTIL P., QUAGLIONI S., STETCU I. and BARRETT B. R., *J. Phys.: Conf. Ser.*, **36** (2009) 083101.
- [9] NAVRÁTIL P., GUEORGUIEV V. G., VARY J. P., ORMAND W. E. and NOGGA A., *Phys. Rev. Lett.*, **99** (2007) 042501.
- [10] ROTH R. and NAVRÁTIL P., *Phys. Rev. Lett.*, **99** (2007) 092501.
- [11] ROTH R., *Phys. Rev. C*, **79** (2009) 064324.
- [12] FRIMAN-GAYER U., ROMIG C., HÜTHER T., ALBE K., BACCA S., BECK T., BERGER M., BIRKHAN J., HEBELER K., HERNANDEZ O. J., ISAAK J., KÖNIG S., PIETRALLA N., RIES P. C., ROHRER J., ROTH R., SAVRAN D., SCHECK M., SCHWENK A., SEUTIN R. and WERNER V., *Phys. Rev. Lett.*, **126** (2021) 102501.
- [13] EPELBAUM E., KREBS H., LEE D. and MEISSNER U.-G., *Phys. Rev. Lett.*, **106** (2011) 192501.
- [14] CALCI A. and ROTH R., *Phys. Rev. C*, **94** (2016) 014322.
- [15] HAUSER W. and FESHBACH H., *Phys. Rev.*, **87** (1952) 366.
- [16] PORTER C. E. and THOMAS R. G., *Phys. Rev.*, **104** (1956) 483.
- [17] HAQ R. U., PANDEY A. and BOHIGAS O., *Phys. Rev. Lett.*, **48** (1982) 1086.
- [18] KOEHLER P. E., BEČVÁŘ F., KRTIČKA M., HARVEY J. A. and GUBER K. H., *Phys. Rev. Lett.*, **105** (2010) 072502.
- [19] GUTTORMSEN M., RAMSØY T. and REKSTAD J., *Nucl. Instrum. Methods Phys. Res. Sect. A*, **255** (1987) 518.
- [20] LARSEN A., SPYROU A., LIDDICK S. and GUTTORMSEN M., *Prog. Part. Nucl. Phys.*, **107** (2019) 69.
- [21] ZEISER F., TVETEN G. M., POTEI G., LARSEN A. C., GUTTORMSEN M., LAPLACE T. A., SIEM S., BLEUEL D. L., GOLDBLUM B. L., BERNSTEIN L. A., BELLO GARROTE F. L., CRESPO CAMPO L., ERIKSEN T. K., GÖRGEN A., HADYNSKA-KLEK K., INGBERG V. W., MIDTBØ J. E., SAHIN E., TORNYI T., VOINOV A., WIEDEKING M. and WILSON J., *Phys. Rev. C*, **100** (2019) 024305.
- [22] TONCHEV A. P., HAMMOND S. L., KELLEY J. H., KWAN E., LENSKE H., RUSEV G., TORNOW W. and TSONEVA N., *Phys. Rev. Lett.*, **104** (2010) 072501.
- [23] ISAAK J., SAVRAN D., KRTIČKA M., AHMED M. W., BELLER J., FIORI E., GLORIUS J., KELLEY J. H., LÖHER B., PIETRALLA N., ROMIG C., RUSEV G., SCHECK M., SCHNORRENBERGER L., SILVA J., SONNABEND K., TONCHEV A. P., TORNOW W., WELLER H. R. and ZWEIDINGER M., *Phys. Lett. B*, **727** (2013) 361.
- [24] ISAAK J., SAVRAN D., LÖHER B., BECK T., BHIKE M., GAYER U., KRISHICHAYAN, PIETRALLA N., SCHECK M., TORNOW W., WERNER V., ZILGES A. and ZWEIDINGER M., *Phys. Lett. B*, **788** (2019) 225 .
- [25] SAVRAN D., ISAAK J., SCHWENGER R., MASSARCZYK R., SCHECK M., TORNOW W., BATTAGLIA G., BECK T., FINCH S. W., FRANSEN C., FRIMAN-GAYER U., GONZALEZ R., HOEMANN E., JANSSENS R. V. F., JOHNSON S. R., JONES M. D., KLEEMANN J., KRISHICHAYAN, LITTLE D. R., O'DONNELL D., PAPST O., PIETRALLA N., SINCLAIR J., WERNER V., WIELAND O. and WILHELMY J., *Phys. Rev. C*, **106** (2022) 044324.
- [26] WELLER H. R., AHMED M. W., GAO H., TORNOW W., WU Y. K., GAI M. and MISKIMEN R., *Prog. Part. Nucl. Phys.*, **62** (2009) 257.
- [27] TAMKAS M., AÇIKSÖZ E., ISAAK J., BECK T., BENOURET N., BHIKE M., BOZTOSUN I., DURUSOY A., GAYER U., KRISHICHAYAN, LÖHER B., PIETRALLA N., SAVRAN D., TORNOW W., WERNER V., ZILGES A. and ZWEIDINGER M., *Nucl. Phys.*, **987** (2019) 79.
- [28] D'ALESSIO A., MONGELLI T., ARNOLD M., BASSAUER S., BIRKHAN J., BRANDHERM I., HILCKER M., HÜTHER T., ISAAK J., JÜRGENSEN L., KLAUS T., MATHY M., VON NEUMANN-COSEL P., PIETRALLA N., PONOMAREV V. Y., RIES P. C., ROTH R., SINGER M., STEINHILBER G., VOBIG K. and WERNER V., *Phys. Rev. C*, **102** (2020) 011302.
- [29] BEUSCHLEIN M., *Nuclear self-absorption with quasi-monochromatic gamma-ray beams for the investigation of the fluctuation of transition widths*, Bachelor Thesis, TU Darmstadt, unpublished (2020).